Materials Science-Poland, 40(1), 2022, pp. 116-129
http://www.materialsscience.pwr.wroc.pl/
DOI: 10.2478/msp-2022-0012

Comparison of spinning trajectory designing methods for products with noncircular cross-section

Marcin Majewski[1,2,*], Tomasz Gądek[1], Leszek Klimek[2], Łukasz Nowacki[1]

[1]Łukasiewicz Research Network – Poznań Institute of Technology, 6 Ewarysta Estkowkiego Street, 61-755 Poznań, Poland

[2]Institute of Materials Science and Engineering, Faculty of Mechanical Engineering, Lodz University of Technology, 1/15 Stefanowskiego Street, 90-924 Łódź, Poland

This article provides information about comparative research on designing of spinning trajectories for products with a noncircular cross-section. Generation of two outlines for the two mandrels was carried out using three methods: (1) a spreadsheet, (2) a 2D CAD program, and (3) a 3D CAD program. Technological tests were carried out using mandrels with the following geometries: ellipse and square. The material used in the research was aluminum Al 1050A. Due to the high degree of complexity in the design of the trajectory, Method 1 was used only for spinning of the ellipse. Methods 2 and 3 were used for spinning the square. Only Method 3 was suitable for programming of upsetting moves of tool. Test of Vickers's microhardness was conducted on sample 3. The influence of the spinning trajectory on the drawpiece was evaluated by measuring the percentage reduction of side wall thickness.

Keywords: *metal spinning, noncircular spinning, asymmetric spinning, sheet metal*

Abbreviations: *ε, strain; x_i, z_i, spinning tool's position in axes x and z; PRT, percentage reduction of side wall thickness; g0, base thickness; g, measured thickness; m, arithmetic average; s, relative standard deviation of the sample.*

1. Introduction

Rotational shaping processes are divided into three main categories: metal spinning, shear forming, and flow forming [1]. The main principle of rotational processes is to make the blank rotate around the spindle axis. Then, by using the designed tools, a stress between yield point and tensile strength is applied to the workpiece [2]. The implementation and development of computerized numerical control (CNC) and stepper motors were key factors in developing an innovative method for spinning noncircular shapes.

The feature that distinguishes noncircular spinning from conventional spinning is the geometric pattern. The cross-sectional geometry of a circle has an infinite number of symmetry axes. This geometric feature allows for the conventional spinning process to be carried out by using the principle of maintaining a constant volume and uniform strain distribution on the cross-section of the blank during the process.

In the case of conventional rotational forming, distribution of strains and stresses is not affected by the position of a forming roller, because the distance between roller and mandrel is always the same. Uniform distribution of stresses by a spin roller in conventional rotational shaping is presented on the left side of Figure 1.

The rotational forming of products with a noncircular cross-section, due to the lack or a limited number symmetry axes, takes place under condition of inhomogeneously arising stresses in the material during the process. The size of the stress heterogeneity depends on the degree of axial asymmetry of the mandrel, as shown on the right side of Figure 1, where different values of stresses will arise depending on the point of contact of the spinning roller with the material. It will cause inhomogeneous strains as: $\varepsilon_1 \neq \varepsilon_2 \neq \varepsilon_3 \neq \varepsilon_4$.

The presented mandrel is a square in cross-section, so it has only four axes of symmetry. This

* E-mail: marcin.majewski@pit.lukasiewicz.gov.pl

© Majewski et al. 2022. This is an open access article distributed under the Creative Commons Attribution-NonCommercial-NoDerivatives 4.0 License. (http://creativecommons.org/licenses/by-nc-nd/4.0/)

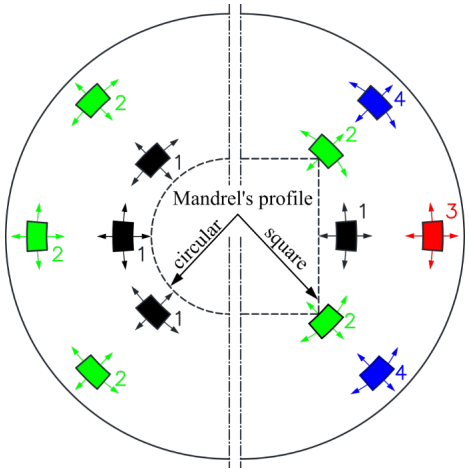


Fig. 1. Strain distribution in rotational forming for circular mandrel (left) and non-circular mandrel (right)

means that the material distribution resulting from its flow due to stresses exceeding R_e in the blank is not the same in all directions. It depends on the degree of asymmetry of the mandrel's geometry. The material flow will occur in privileged directions, which will depend on several conditions, such as the geometry of the blank, type of material, and strain hardening.

An additional factor that hinders the analyses of the material flow in the semi-finished product during the axially asymmetric rotational forming is the complexity of the kinematics of the spinning process, in which two opposing phenomena occur simultaneously: material compression in the circumferential direction and stretching in the radial direction.

2. Analysis of the literature

Publication [3] from 1975 indicates that experiments involving spinning of axially asymmetrical products were conducted as early as during the 1970s. The probable reason why this technology was not propagated was the lack of technical capabilities, particularly with regard to CNC control and the drives applied. The spinning process shown in Figure 2 is performed using a mandrel with a square cross-section and a spinning tool being a negative of the mandrel.

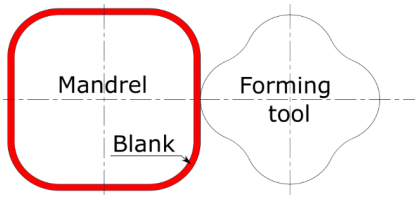


Fig. 2. Diagram of spinning a noncircular cross-section [3]

Analysis of the literature indicates that, for the purposes of developing asymmetrical spinning, work on designing a spinning lathe adapted to this process was started. The condition for performing effective spinning was to ensure that the roll would not collide with the mandrel, which had a noncircular cross-section. Arai [4] described the design of an innovative spinning lathe designed for spinning of axially asymmetrical products with the application of control via the force generated on the spinning roll. Studies indicate that a substantial step change in the pressing force of the forming roll occurs at the site where the mandrel's geometry changes from curvilinear to planar. A different concept of a spinning lathe for axially asymmetrical products can be found in Ref. [5], where the process kinematics involve synchronization of the moving spinning roll in one direction (left–right) and of the moving template in the direction perpendicular to the roll's direction (front–back). During tests, the influence of asymmetry of the spun shape's geometry on the distribution of stresses during the process was noted. It was determined that radial stresses change with the angle of rotation of the elliptical mandrel. Stresses grow as the mandrel's angle of rotation changes and the spinning tool approaches the longer axis of the ellipse, and decreases when the spinning tool approaches the shorter axis of the ellipse. A similar phenomenon was observed in studies of spinning an axially asymmetrical cone in die-less spinning. Jia et al. [6] noted a significant effect of the half-cone angle. Forming a smaller half-cone angle resulted in a more uniform material hardening. According to the authors, this was due to the fact that when forming a smaller half-cone angle, the pressure exerted by the roller increased. While form-

ing the largest half-cone angle leads to the largest differences in material hardening of up to 15%. A similar composition and its results were published in their next article [7]. Instead of the surface hardening effect, the article this time analyzed the phenomenon of nonuniform deformation during spinning of axially unsymmetrical products. The authors conducted FEM studies which they compared with real trials. Research has shown that the greatest deformation of the material takes place in the 0° area, and the smallest takes place in the 180° area. This confirms the strong correlation between the asymmetry of the product and the deformation of the material.

Another approach to spinning lathe design was presented in article [8], where a constant pressing force was applied with a constant gap. It was noted that the system of spinning control via spinning roll pressing force has flaws when applied to axially asymmetrical spinning, due to differing forming conditions in the case of convex and concave mandrel geometries. It was indicated that applying the axially asymmetrical spinning method with a constant distance between the mandrel and spinning roll not only eliminates problems arising from differing forming conditions between convex and concave geometries but also enables the researcher to adjust the spinning trajectory. Sugita and Arai [9] used a spinning lathe equipped with a force meter mounted on the spinning tool, which was used to generate the trajectory of the spinning tool via force measurement. During spinning of an axially symmetrical shape, 5% wall thinning occurred, but during spinning of an axially asymmetrical shape with a square cross-section, the thinning amounted to as much as 50% of the initial thickness, with a measured tendency of material accumulation in the right angles (corners) of the detail.

Advances in technology and CNC control afforded researchers with the appropriate laboratory equipment with the opportunity to study axially asymmetrical spinning, and they began to focus more on studying the spinning trajectory in axially asymmetrical products, with article [10] being evidence of this. Focus was placed on the theory concerning designing of the spinning roll's trajectory in the process of spinning without a mandrel in easily deformable 1050-grade aluminum, with a thickness of 2 mm. The applied algorithm for designing and generating the spinning tool's trajectory was made using the MATLAB® software. Drawpieces with wall thinning of $\approx 15\%$ were produced, where the greatest scatter in thickness measurement was noted in the corners of the drawpiece. Also, in 2020, Arai and Gondo [11] described the results of their research in the scope of designing spinning trajectories.

Designing product trajectories for axially unsymmetrical products is an important stage in production. Loukaides and Russo [12], in their analysis of the design of trajectories for metal spinning, indicated that most studies and recommendations concern shear forming, and not metal spinning. This is due to the very difficult nature of metal spinning. Numerous studies on trajectory design for axially symmetric products indicate that the material should be formed in multiple steps to prevent folding. The authors' analysis also shows that the spinning trajectory will largely depend on the feed per revolution parameter. In the current state of knowledge, it should be assumed that the recommendations for the design of the spinning trajectory for the spinning of axially symmetrical products can only partially be applied to axially unsymmetrical products. Many works indicate that designing a toolpath for metal spinning can be supported by FEM analyses, especially in such cases as multipass forming [13], rotational shaping of stainless steel [14], and rotational shaping without using a die [15]. Although the acquired results can be very accurate, conducting FEM analyses is time-consuming.

Due to the low popularity and research nature of axially asymmetric spinning, no extensive knowledge base about the theoretical foundations of the process was established. Therefore, for the analysis of shaping conditions, reference was made to the related literature describing rotational shaping in terms of the analysis of the kinematics of the process. The analyzed literature [16] distinguishes two methods of defining stresses and strains in rotational shaping: analytical and numerical. Analytical methods are based on four basic models: (1) deformation energy method [17], (2) the up-

per bound method [18], (3) prediction of failure by wrinkling [19], and (4) predictions of strains in spinning [20]. Analytical methods for describing the forces in rotational shaping have been described and developed at least since the 1950s, while numerical methods were developed only in the early 1990s [21]. Due to the limitations of the computing power of modern computer units, the first models were very simplistic. The vast differences in the FEM analyses result from the division into implicit [22] and explicit methods [23]. The analyzed literature in the aspect of predicting the stress distribution in the spinning of axially symmetrical products shows that hoop stresses are the smallest and have the lowest impact on the shaped detail. The carried out tests of axially unsymmetrical spinning indicate that hoop stresses have a much greater influence on the process than in axially symmetrical spinning. However, this issue requires further research.

Analysis of the literature indicates that many authors, in their works [4, 5, 7, 8, 24], refer to the rotary forming process of axially asymmetrical products as spinning, while the trajectory and character of the process applied by them have more features similar to shear forming than metal spinning. A characteristic feature of shear forming is that it occurs in one motion, which forms the side wall to the planned thickness arising from the formula. Shear forming introduces only tensile stress. The spinning process takes place in several movements and may consist of movements introducing both compressive and tensile stresses or solely tensile stresses. In effect, the obtained thickness of the drawpiece will be a resultant of the stresses introduced, while the side wall thickness reduction is an unintended effect. A comparison is shown in Figure 3. It should be emphasized that this linguistic error does not arise from the bad faith of the authors, but from the fact that spinning of products with a noncircular shape has been the subject of research for a relatively short time. Designing a trajectory that introduces only tensile stresses is easier to do as it does not require such expansive CNC code.

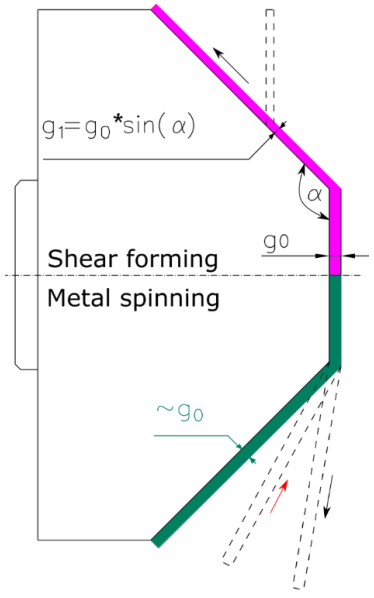


Fig. 3. Diagram comparing shear forming and metal spinning

3. Goal of research

The goal of the tests presented in this article is to develop innovative methods of designing spinning trajectories for noncircular products and to determine the influence of trajectory on the height of the drawpiece obtained, with particular differentiation between spinning and shear forming of a product with a noncircular cross-section. Two mandrels were used for tests with the purpose of designing a spinning trajectory: (1) in the shape of an ellipse with dimensions of 60 mm × 80 mm and (2) in the shape of a square with dimensions of 80 mm × 80 mm. CAD models are presented in Figures 4 and 5. Designed trajectories were tested by metal spinning blanks made from aluminum Al 1050 A. The strength of the material was measured at three angles to the rolling directions of aluminum sheet. The properties are presented in Table 1.

Table 1. Strength of material depending on angle-to-rolling direction

Angle (°)	**$R_{p0.2}$ (MPa)**	**R_m (MPa)**	**A_{80mm} (%)**
0	37.0	72.7	47.2
45	38.6	78.9	46.7
90	37.5	68.9	53.3

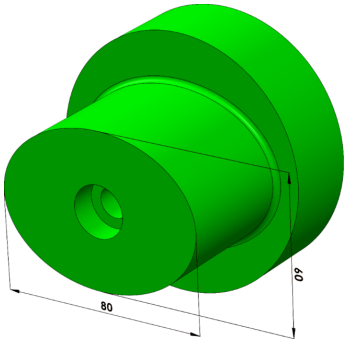


Fig. 4. Mandrel in the shape of an ellipse with dimensions 60 mm × 80 mm

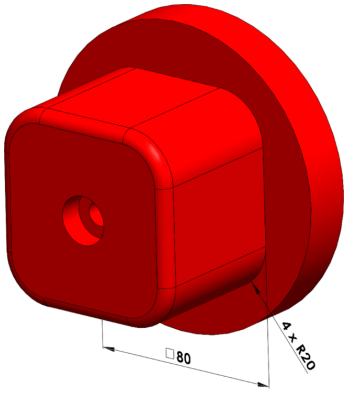


Fig. 5. Mandrel in the shape of a square with dimensions 80 mm × 80 mm

The first step in designing a spinning trajectory using CNC code controlling the position of the spinning tool is to acquire a set of points coordinating the position of the spinning tool according to the mandrel's outline as a function of the mandrel's angle of rotation as: $f(\alpha) = x_i, z_i$, where α is the angle of the mandrel's rotation in degrees, and x_i and z_i are the positions of the spinning tool. During tests, three methods were used for this purpose: (1) using a spreadsheet and mathematical formulas, (2) using 2D CAD software, and (3) using 3D CAD software and an algorithm generating the trajectory. Conducted tests indicated that all the three methods make it possible to generate the mandrel's outline as a function of the mandrel's angle of rotation around the spindle's axis. The number of control commands depends directly on the complexity of the mandrel's shape and the required resolution. It should be accepted that the minimum number of points required for generating the trajectory of a single movement is 1 g-code command per 1° of the mandrel's rotation. To perform a full 360° rotation, 360 commands synchronizing the roll's position with that of the mandrel are required.

Method 1, utilizing mathematical formulas and spreadsheets to describe the mandrel's outline, is the most difficult and time-consuming method due to the fact that the trajectory must consist of an appropriately high resolution of manually generated coordinating points. During spinning of axially asymmetrical products, it is necessary to perform multiple mandrel revolutions synchronized with the advance rate of the spinning roll on the x and z axes. The complexity of the spinning trajectory's CNC code increases as per the product: 360 commands × number of revolutions. This product means that a single movement of the spinning tool requires ≈ 75,000 g-code lines to obtain a drawpiece with a noncircular cross-section in the shape of an ellipse on mandrel no. 1 from Figure 4. Over 300 000 g-code lines were used in total to obtain the drawpiece. Due to its complexity, this method requires the creation of five separate trajectories of the spinning tool's motion, in which the spinning tool performs spinning movements that stretch the material and position the piece's side wall at angles of 18°, 30°, 45°, 68°, and 90°, according to Figure 6. The goal of these tests was to produce a drawpiece with a height of 30 mm.

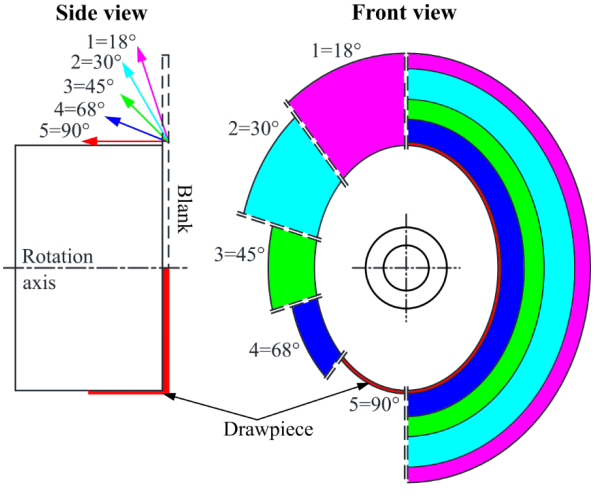


Fig. 6. Trajectories of spinning movements: ellipse

The second method of designing the spinning trajectory was to apply the 2D CAD software. This method requires the application of a model in which the cross-section of a noncircular mandrel, having precisely one degree of freedom, namely, its rotation around its axis, which, under real-life conditions, will be co-linear with the axis of the spinning lathe's spindle. The mandrel's outline must be found in a relation of continuous contact with the model of the spinning roll. Next, the x_i and z_i position parameters must be noted manually depending on the mandrel's angle of rotation. This is a time-consuming method, but in contrast to the method based on the use of spreadsheets, it is more flexible and easier to apply to cross-sections with more geometrically complex shapes. The method was applied to produce the piece on mandrel no. 2, with a square cross-section according to the model in Figure 5. Over 168 000 g-code lines were used in total to obtain the drawpiece. Due to its complexity, this method requires the creation of five separate trajectories of the spinning tool's motion, in which the spinning tool performs spinning movements that stretch the material and position the piece's side wall at angles of 25°, 30°, 45°, 68°, and 90° according to Figure 7. The goal of these tests was to produce a drawpiece with a height of 30 mm.

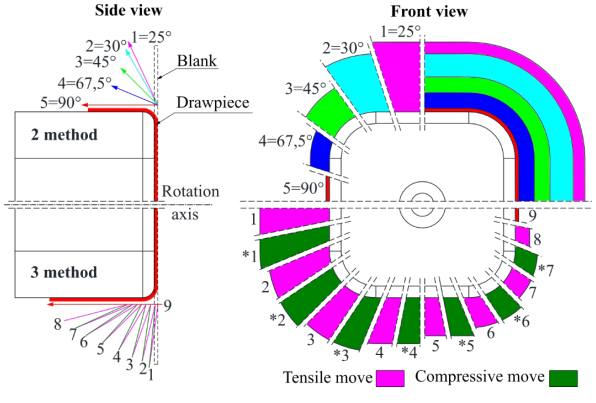


Fig. 7. Trajectories for mandrel square: Method 2 at the top of the picture and Method 3 at the bottom of the picture

Method 3, utilizing 3D CAD software, is the most advanced method of obtaining the set of points describing the contour of points as a function of the mandrel's rotation. This method was used to design a spinning trajectory consisting of both movements stretching the material and upsetting the material. Introducing such a solution will make it possible to obtain drawpieces of a greater height. Methods 1 and 2 made it possible to obtain drawpieces with a height of 30 mm, and the application of Method 3 made it possible to obtain drawpieces with a height >40 mm.

The application of the method utilizing the outline of 3D CAD mandrel models made it possible to increase the number of spinning movements from 5 to 17, while simultaneously reducing the spinning trajectory to ≈ 1,000 commands in g-code. An additional advantage of this method is that it allowed for programming of movements stretching the material (marked in Figure 7 in red) and also movements compressing the material (marked in Figure 7 in green). The movements marked in Figure 7 from 1 to 8 consist of stretching and upsetting movements, while the final movement, 9, is a movement pressing the material to the mandrel. The previous methods required the creation of separate programs for performing a single movement and took up hundreds of thousands of lines, while this method makes it possible to perform more movements of the spinning tool with a much lesser volume of CNC code.

4. Research methodology

Tests of spinning products with noncircular cross-sections were performed on a spinning lathe MWS-200, equipped with step motors and a spindle allowing for precise control of the mandrel's rotations. The control system of the MWS-200 synchronizes the position of the spinning roll, making it possible to avoid collision between the roll and the mandrel.

Tests were performed on two mandrels with the use of three methods of designing the spinning trajectory. The geometry of the produced drawpieces was tested using a micrometer for measurement of the thickness of the drawpiece walls. At least 10 drawpieces were made by each method. The thickness of the blanks was from 1.5 mm to 2.5 mm.

Mandrel no. 1 – ellipse, on which spinning was performed with the spinning trajectory generated

by Method 1. The dimensions of the ellipse-shaped blank were 120 mm × 95 mm. The thickness of the ellipse drawpiece was measured at three sites: the semi-minor axis – point A and the semi-major axis – point C of the ellipse, and at the center between them – point B. Measurements were taken after every spinning operation at angles 18°, 30°, 45°, 68°, and 90° at a distance of 15 mm from the frontal area of the drawpiece.

Mandrel no. 2 – the square shown in Figure 5, on which spinning tests were performed using Methods 2 and 3. The scheme of wall thickness measurements consistent with Figure 8 was applied to the square drawpiece.

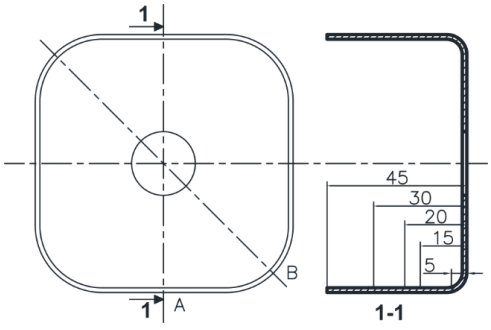


Fig. 8. Measuring sites A and B on the square drawpiece

Measurements were taken at two sites: measurement A – on the flat wall and measurement B – on the rounded corner of the drawpiece. The height at which measurements were taken was based on the diagram in Figure 8; side wall thickness measurement was performed at the following distances from the face of the drawpiece: 5 mm, 15 mm, and 30 mm. The dimensions of the square-shaped blank were: 140 mm × 140 mm for Methods 2 and 3.

Based on the performed thickness measurements of the side walls of the drawpieces obtained, the relative percentage reduction of wall thickness (PRT) following each spinning process was calculated. Thinning was calculated based on Eq. (1) as

$$PRT = \left(1 - \frac{g}{g_0}\right) \times 100\% \qquad (1)$$

The spun drawpieces were scanned on the ATOS COMPACT SCAN 5M mobile optical scanner. In the dedicated GOM INSPECT V8 Professional software, the scanned shapes of the drawpieces were compared with the CAD models and the deviation was shown in the form of a figure.

5. Test results

5.1. Method 1

Spinning of the ellipse drawpiece was carried out by performing five trajectories consistent with Figure 6. After the completion of each trajectory, the thickness of the drawpiece's side wall was measured. Next, the drawpiece was mounted on the MWS-200 spinning lathe, and the process was continued using the next trajectory. The results of side wall thickness measurements for ellipse drawpieces spun using the trajectory generated by Method 1 are given in Table 2. Average values are given in the column under the *m* symbol, and standard deviation values are given under the *s* symbol. The explanation and location of the measurement sites is described in the section "Research methodology."

Analysis of the results given in Table 2 indicates that the PRT value is low for angles 18°, 30°, and 45°. A substantial increase occurs during forming at the angles of 68° and 90°. The results indicate that PRT for sites A, B, and C for angles 18° and 30° is at a similar level. It was observed that, for angles 45° and 68°, PRT is lower at measurement site C than at other sites of measurement. This is not a constant dependency, and during forming at the angle of 90°, PRT at every measurement site differs and grows in the following manner: A < B < C.

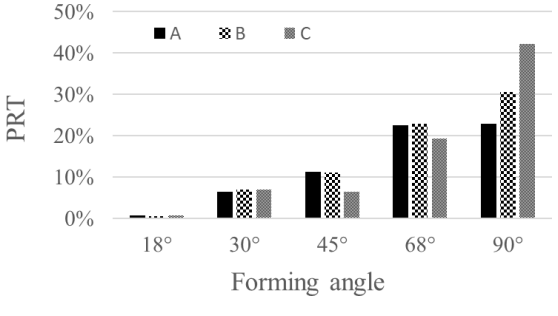


Fig. 9. Chart of average *m* values depending on forming angle: Method 1

Table 2. Thickness measurements: ellipse, 15 mm from frontal area

Item no.	Angle (°)	Measurement	PRT						*m*	*s*
		A	0.5%	0.5%	1.0%	1.0%	0.5%	0.5%	0.7%	0.00
1	18	B	0.5%	0.5%	0.5%	1.0%	1.0%	0.5%	0.7%	0.00
		C	0.0%	1.0%	0.5%	1.0%	1.0%	1.0%	0.8%	0.00
		A	4.5%	8.0%	8.5%	6.5%	7.0%	4.5%	6.5%	0.02
2	30	B	5.0%	8.5%	8.5%	7.0%	8.0%	5.5%	7.1%	0.02
		C	4.0%	10.5%	9.5%	7.5%	6.5%	5.0%	7.2%	0.03
		A	13.0%	14.0%	14.5%	12.0%	9.5%	4.5%	11.3%	0.04
3	45	B	15.5%	14.0%	12.5%	10.0%	9.5%	6.0%	11.3%	0.03
		C	7.5%	8.5%	7.5%	7.0%	5.5%	3.5%	6.6%	0.02
		A	13.5%	22.5%	29.0%	28.5%	22.5%	19.5%	22.6%	0.06
4	68	B	19.5%	30.0%	30.0%	22.5%	18.5%	17.0%	22.9%	0.06
		C	17.5%	28.5%	27.5%	19.5%	12.0%	11.5%	19.4%	0.07
		A	14.0%	22.0%	34.0%	35.5%	21.0%	10.5%	22.8%	0.10
5	90	B	26.0%	35.0%	44.0%	38.5%	24.5%	16.5%	30.8%	0.10
		C	51.0%	55.5%	51.5%	47.5%	36.5%	11.5%	42.3%	0.16

PRT, reduction of wall thickness

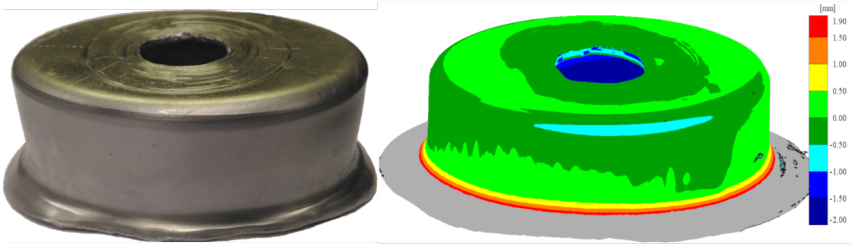


Fig. 10. Drawpiece in the shape of an ellipse

The average PRT value results from Table 2 are shown in Figure 9.

The chart shown in Figure 9 indicates that, up to the forming angle of 30°, the axial asymmetry of the ellipse does not affect the PRT value; however, forming at the angles of 45° and 68° causes a higher PRT increase at sites A and B. The chart indicates that, for the angle of 90°, a substantial PRT increase occurred at site C, while the PRT at site A did not change significantly.

It is possible to generate a spinning trajectory using mathematical formulas and a spreadsheet; however, practical tests show that generating a spinning trajectory using this method is both difficult and time-consuming. For technological reasons, to avoid collision between tools, much care must be taken, and potential modification of the trajectory requires much caution. Generating a single spinning movement took ≈ 16 work hours, which meant that, in effect, carrying out technological tests of ellipse spinning with the application of five movements required about 80 work hours. The ready product is shown in Figure 10.

In addition, it should be emphasized that spinning consisted of separate spinning programs. The high degree of complexity involved in generating a trajectory by means of Method 1 made it impossible to generate movements upsetting the material, which resulted in significant thinning in the final movement.

5.2. Method 2

In the next step, spinning of square drawpieces was carried out using the trajectory generated by Method 2. The spinning process consisted of five trajectories according to Figure 7, which were initiated manually in succession. The results of the

Table 3. Thickness measurements for the square drawpiece spun by Method 2

Height (mm)	Measurement	PRT				*m*	*s*
5	A	9.3%	14.7%	13.3%	13.3%	12.7%	0.02
	B	0.0%	7.3%	6.0%	8.0%	5.3%	0.04
15	A	39.3%	50.7%	45.3%	38.0%	43.3%	0.06
	B	26.7%	36.7%	39.3%	40.0%	35.7%	0.06
30	A	44.7%	68.0%	10.7%	6.7%	32.5%	0.29
	B	45.3%	50.0%	51.3%	49.3%	49.0%	0.03

PRT, reduction of wall thickness

Table 4. Thickness measurements for the square drawpiece spun by Method 3 (negative values are the result of compressive strains of the material)

Height (mm)	Measurement	PRT				*m*	*s*
5	A	−1.2%	−1.5%	−1.4%	−1.6%	−1.4%	0.00
	B	−6.0%	−2.0%	−3.2%	−1.2%	−3.1%	0.02
15	A	5.7%	5.7%	4.0%	12.0%	6.8%	0.04
	B	6.8%	0.4%	7.2%	8.8%	5.8%	0.04
30	A	2.0%	2.8%	4.8%	2.0%	2.9%	0.01
	B	8.8%	6.0%	8.4%	2.8%	6.5%	0.03
45	A	2.0%	2.8%	4.8%	2.0%	2.9%	0.01
	B	−1.6%	1.2%	−0.4%	0.0%	−0.2%	0.01

PRT, reduction of wall thickness

thickness measurements are given in Table 3.

Analysis of the PRT results given in Table 3 indicates that, at a height of 5 mm from the face of the drawpiece, PRT at site A on the planar surface is nearly two times greater than in the corner rounded with an R20 radius. As the distance of measurement increases to 15 mm, that is, half of the drawpiece's height, a higher PRT value is maintained at site A. A reversal of this dependency, that is, PRT being greater at site A than at site B, occurs at the 30 mm distance of measurement, that is, at the end of the drawpiece. *m* value results for the square drawpiece spun according to Method 2 are shown on the chart in Figure 11.

The chart of average *m* values from Table 3, for Method 2, indicates that there is a significant divergence in PRT between the heights of 15 mm and 30 mm. Despite the fact that no upsetting movements were applied in this method, PRT for site A is subject to reduction from a value >40% to >30% between the height of 15 mm and 30 mm. Most likely, at the height of 30 mm, material from the corners flowed in the direction of the planar surfaces at site A.

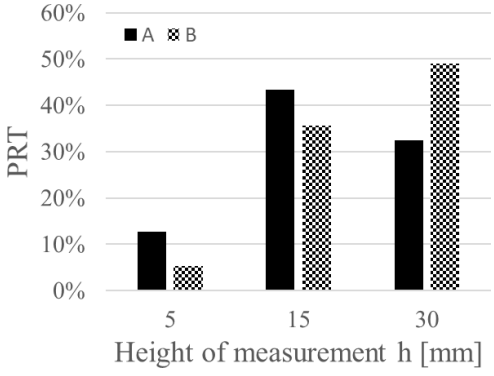


Fig. 11. Chart of average m values depending on forming angle: Method 2

Expansion of the spinning trajectory designing method with the use of 2D CAD software facilitated and accelerated the process of generating spinning trajectories by ≈ 50%. The implemented solution made it possible to generate a spinning trajectory for a mandrel that was more difficult to describe using mathematical formulas, since the cross-section of a square consists of flat surfaces and rounded corners, which, in the case of Method

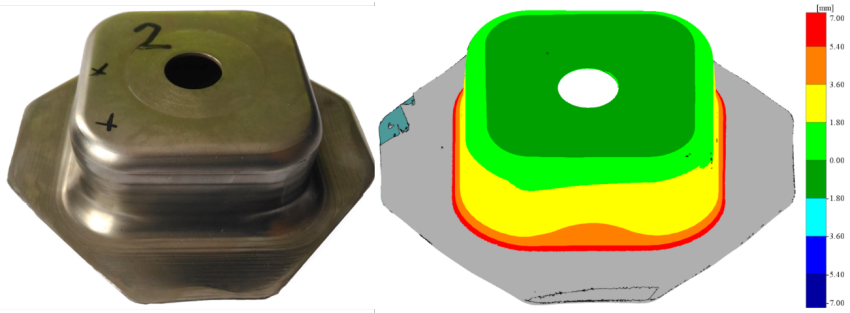


Fig. 12. Drawpiece in the shape of a rectangular obtained by Method 2

1, requires the application of a separate formula. Drawpieces obtained using Method 2 are shown in Figure 12.

The application of 2D CAD software made it possible to eliminate this problem. In effect, generating a single spinning movement lasted 9 work hours, and in total, 45 work hours were required to generate five movements.

5.3. Method 3

Spinning tests using Method 3 were carried out using a single program generating 17 spinning movements alternatingly applying tensile and compressive strains to the material according to Figure 7. The results of thinning of the material of the square drawpieces obtained using Method 3 are given in Table 4.

The results of side wall thickness measurements indicate that wall thickness in the case of the square drawpiece is nonuniform for the flat surface of measurement site A. At the same time, in wall thickness measurements at measuring site A, at a height of 30 mm, the highest standard deviation value occurs. This indicates that wall thickness at this site depends on many factors, such as: radius of the spinning roll, mandrel geometry, and rate of advance per revolution. The results are presented on the chart in Figure 13.

Spinning with the application of Method 3 made it possible to introduce movements that compress the material during the process, and this has a positive effect in the form of low PRT values, which do not exceed 7%. The introduced compressive movements caused the material to be upset and

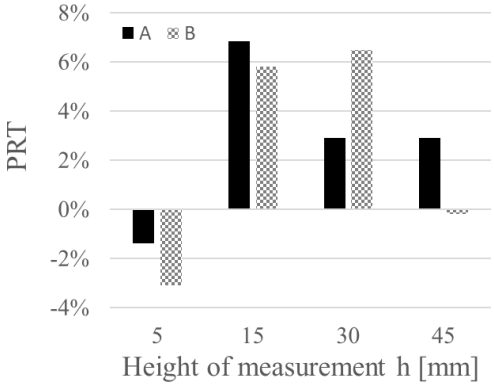


Fig. 13. Chart of average m values depending on forming angle: Method 3

PRT values to be negative at a distance of 5 mm from the face of the drawpiece. The chart shows that, at a height of 30 mm, PRT at site B is nearly two times greater than at site A. At the measuring height of 45 mm, PRT at site A amounts to $\approx 3\%$, and at site B, $\approx 0\%$. Analysis of the chart indicates that Method 3, by introducing compressive movements, made it possible to maintain PRT at a similar value in the corners of the square at site B. The drawpiece obtained by Method 3 is shown in Figure 14.

The applied method, utilizing 3D CAD software, not only significantly facilitated the process of generating the spinning trajectory, but also made it possible to introduce movements upsetting the material. In effect, sites where the drawpiece's thickness is greater than the blank's thickness are found in the tested cross-sections. This effect was observed at a height of 5 mm and 45 mm. Meanwhile, thinning amounted to $\approx 5\%$ at the draw-



Fig. 14. Square drawpiece obtained by Method 3

piece height of 15 mm and 30 mm. Generating a trajectory by means of Method 3 made it possible to reduce the volume of CNC code and accelerated the process of generating it. Also, generating the trajectory took approx. Twenty-four work hours, which is a time nearly half of that required by Method 2. Method 3 made it possible to obtain a drawpiece $\approx 50\%$ higher with a more uniform wall thickness.

From the drawpiece made by Method 3, two samples were collected for microhardness testing by the Vickers method conducted with Micromet 2104 with loading force 0,9807 N in time 13 s. In sample 1 microhardness was measured from spot 1, with a 2 mm step, until spot 45. The sample was taken at 15 mm from the face of the drawpiece. On sample 1 a distance of 6 mm thickness was measured by a microscope. The visualization of microhardness test spots in sample 1 is presented in Figure 15. Sample 2 was taken from the drawpiece cross section.



Fig. 15. Visualization of measured hardness points in sample 1

The microhardness was tested on a flat surface and on a surface rounded with an R20 radius. A metalographic transverse section was made and microhardness measurements were made. The obtained results are shown in Figure 16.

The microhardness results up to a distance of 15 mm presented in Figure 16 show the hardness of the flat surface. Above the height of 15 mm, the hardness measurement begins in the section rounded with the R20 radius. The graph shows that as the spinning tool approached the rounded part, the hardness increased. This indicates that the tool strengthened the first-half of the arc more, and above the distance of 35 mm, the tested surface hardness decreased. This indicates a heterogeneous material hardness distribution, which is strongly dependent on the pattern geometry.

Figure 16 shows an auxiliary graph for the drawpiece thickness measurements. Measurements show that on a flat surface at a distance from 1 mm to 23 mm, the material thickness increases. After reaching the local extreme, the wall thickness is reduced to a distance of 42 mm. Measurements show unusual material behavior during processing. Compared with spinning an axially symmetrical product, the material thickness and the peripheral hardness should be uniform. The performed measurements show that there is no such relationship in the axially asymmetric spinning. Measurements show that flat surfaces have a lower material thickness and lower hardness, while at the point where the surface passes into the arc, the material thickness and hardness increase. This is contrary to the expected situation, where an increase in the hardness

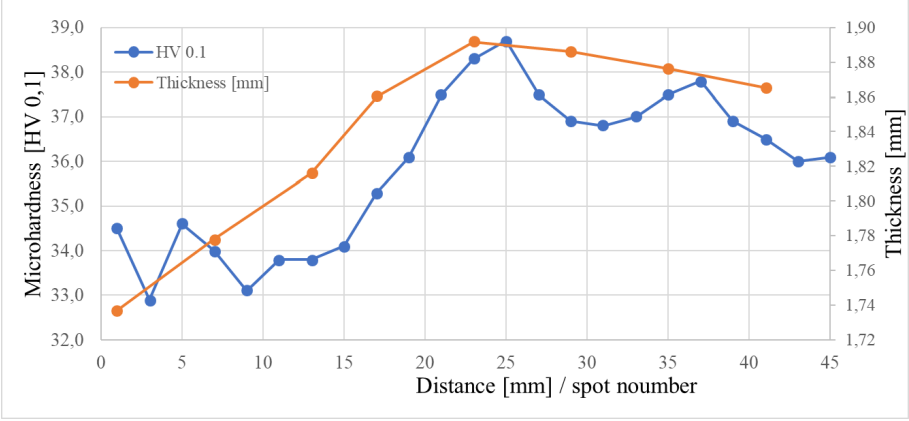


Fig. 16. Hardness Vickers HV 0,1 near the surface

of the material would cause a greater thinning of the material. The above observations indicate that the spinning tool significantly compresses the material and forces it to move in the circumferential direction. The above observation is correct for the first quarter of the arc, since the local maximum hardness occurs around this point. Then the hardness and thickness of the material are lowered in the further part of the arch. These results confirm the observation made in [6].

Microhardness in sample 2 was measured from the outer surface, that is, the contact of the roller with the material to the internal surface, which is the contact between the material and the mandrel. Between the outer and inner surfaces, seven measurements of the microhardness were made at a distance of about 0.20 mm. The hardness on the outer surface was 39.8 HV, and the hardness on the inner surface was 32.3 HV. The hardness distribution on the cross-section was close to linear.

6. Conclusions

Conducted tests of designing and generating a spinning trajectory for axially asymmetrical products led to the following conclusions:

1. It is possible to spin simple, axially asymmetrical shapes using Method 1; however, this is a time-consuming and complicated process. This means that, in laboratory conditions of testing, it is very difficult to implement and can only be applied in the case of simple shapes whose geometry can easily be described with a single mathematical formula in a Cartesian coordinate system. Also, this method was not suitable to apply compressive moves.
2. Method 2 is somewhat easier and makes it possible to save time on designing the spinning trajectory; however, its greatest advantage is that it substantially facilitates designing of the spinning trajectory in the case of geometries that cannot be described by a single mathematical formula in a Cartesian coordinate system.
3. Method 3 is the fastest method of generating a spinning trajectory, and at the same time, the simplest one. The advantage of this method with respect to Method 2 is a reduced time of designing the spinning trajectory and the lesser volume of CNC code. The simplicity of this method makes it possible to easily introduce movements compressing the material, which has a favorable impact on the thickness and height of the drawpiece.
4. Tests confirmed the hypothesis of nonuniform strains distribution depending on the mandrel's geometry. This can be seen in the ellipse drawpiece. PRT changes at individual heights of measurements between sites A and B. Spinning tests indicate that

the greater is the side wall forming angle, the more nonuniform the flow of material. A similar phenomenon was observed in the square drawpiece spun according to Method 2.

Compliance with Ethical Standards

This study was funded by Łukasiewicz Research Network – Metal Forming Institute, number of project BT.901.0113

Conflicts of interest

The authors declare that they have no conflicts of interest.

Ethical approval

This article does not contain any studies with human participants or animals performed by any of the authors.

Acknowledgements

We are grateful for Mr. Michał Pieszak's contribution to the research.

References

[1] Runge M. Spinning and flow forming: spinning and flow forming technology, product design, equipment, control systems. Radevormwald: Lippert Druck GmbH; 1993.

[2] Grainger JA. The flow turning of metals. Eastbourne and London: The Machinery Publishing Co. Ltd.; 1969.

[3] Meshcherin VT. Listovaya Shtampovka. Moskva: Mashinostroyenie; 1975.

[4] Arai H. Force-controlled metal spinning machine using linear motors. Proc IEEE Int Conf Robot Autom. 2006;2006:4031–6. https://doi.org/10.1109/ROBOT.2006.1642321.

[5] Shimizu I. Asymmetric forming of aluminum sheets by synchronous spinning. J Mater Process Technol. 2010;210:585–92. https://doi.org/10.1016/j.jmatprotec.2009.11.002.

[6] Jia Z, Han Z, Liu B, Xiao Y. Work hardening of non-axisymmetric die-less spinning. J Mech Eng. 2017;63:111–8. https://doi.org/10.5545/sv-jme.2016.3589.

[7] Jia Z, Han ZR, Liu BM, Fan ZJ. Numerical simulation and experimental study on the non-axisymmetric die-less shear spinning. Int J Adv Manuf Technol. 2017;92:497–504. https://doi.org/10.1007/s00170-017-0172-x.

[8] Awiszus B, Härtel S. Numerical simulation of non-circular spinning: a rotationally non-symmetric spinning process. Prod Eng. 2011;5:605–12. https://doi.org/10.1007/s11740-011-0335-9.

[9] Sugita Y, Arai H. Formability in synchronous multipass spinning using simple pass set. J Mater Process Technol. 2015;217:336–44. https://doi.org/10.1016/j.jmatprotec.2014.11.017.

[10] Polyblank JA, Allwood JM. Parametric toolpath design in metal spinning. CIRP Ann Manuf Technol. 2015;64:301–4. https://doi.org/10.1016/j.cirp.2015.04.077.

[11] Arai H, Gondo S. Oblique/curved tube necking formed by synchronous multipass spinning. Metals. 2020;10:733. https://doi.org/10.3390/met10060733.

[12] Loukaides EG, Russo IM. Toolpath generation for asymmetric mandrel-free spinning. Procedia Eng. 2017;207:1707–12. https://doi.org/10.1016/j.proeng.2017.10.926.

[13] Rentsch B, Manopulo N, Hora P. Numerical modelling, validation and analysis of multi-pass sheet metal spinning processes. Int J Mater Form. 2017;10:641–51. https://doi.org/10.1007/s12289-016-1308-5.

[14] Yaman K, Özcan M, Tekiner Z. Determination of the spinning parameters of AISI 304L stainless steel by using finite element method. J Fac Eng Archit Gazi Univ. 2018;33:299–311. https://doi.org/10.17341/gazimmfd.406802.

[15] Sedighi M, Jalili I, Kasaeian-Naeini M. Experimental study and FEM analysis of forward hot dieless spinning. Mechanics and Industry 2018;19. https://doi.org/10.1051/MECA/2018034.

[16] Music O, Allwood JM, Kawai K. A review of the mechanics of metal spinning. J Mater Process Technol. 2010;210:3–23. https://doi.org/10.1016/J.JMATPROTEC.2009.08.021.

[17] Wang Q, Wang T, Wang ZR. A study of the working force in conventional spinning. In: Proceedings of the Fourth International Conference of Rotary Forming, 1989, pp. 103–8.

[18] Kim JH, Park JH, Kim C. A study on the mechanics of shear spinning of cones. J Mech Sci Technol. 2006;20:806–18. https://doi.org/10.1007/BF02915944.

[19] Hayama M, Murota T, Kudo H. Deformation modes and wrinkling of flange on shear spinning. Bull Japan Soc Mech Eng. 1966;9:423–33. https://doi.org/10.1299/JSME1958.9.423.

[20] Quigley E, Monaghan J. Metal forming: an analysis of spinning processes. J Mater Process Technol. 2000;103:114–9. https://doi.org/10.1016/S0924-0136(00)00394-0.

[21] Alberti N, Cannizzaro L, Lo Valvo E, Micari F. Analysis of metal spinning processes by the ADINA code. Comput Struct. 1989;32:517–25. https://doi.org/10.1016/0045-7949(89)90343-X.

[22] Lu XY, Zhang S, Hou H, Li JZ, Zhou LX, Li ZQ. Three dimensional fe analysis on flange bending for TC4 alloy during shear spinning. J Mater Sci Technol. 2006;22:855–9.

[23] Zhan M, Yang H, Zhang JH, Xu YL, Ma F. 3D FEM analysis of influence of roller feed rate on forming force and quality of cone spinning. J Mater Process Technol. 2007;187–188:486–91. https://doi.org/10.1016/

j.jmatprotec.2006.11.114.

[24] Xia QX, Lai ZY, Long H, Cheng XQ. A study of the spinning force of hollow parts with triangular cross sections. Int J Adv Manuf Technol. 2013;68:2461–70. https://doi.org/10.1007/s00170-013-4847-7.

Received 2022-02-11
Accepted 2022-05-20